# Multi-fidelity drag prediction for base bleed projectile



# Multi-fidelity drag prediction for base bleed projectile

**M MAziz[1], AZ Ibrahim[1,2], M Y M Ahmed[1] and A M Riad[1]**
[1] Mechanical Engineering Branch, Military Technical College, Kobri El-Kobba, Cairo, Egypt.
[2] Corresponding author, Email: **a.ibrahim@mtc.edu.eg.**

**Abstract**. A computational study is performed to predict the drag reduction for a base bleed projectile. 2-D and 3-D simulations are conducted to describe the flow past a projectile with base bleed. The calculated computational results are compared with measurements of total drag coefficients based on published results for 155mm K307 projectiles with live/dummy base bleed grain. In addition, the mean drag coefficient measurements based on live firing tests for a five K307 projectiles with live BB grain at different Mach numbers are used to validate results obtained from the computational results. Differences between the drag coefficient calculated from computational and published live firing measurements of the drag coefficient for K307 are less than 5.2% and 6.8% for projectile with dummy and live BB, respectively. On the other hand, the maximum deviation between computational results and real measurements from the live firing tests of live BB projectiles is 2.75%.

## 1. Introduction

Since the upper hand in battle for those with highest range of ammunition, most countries are rushing to find various ways to increase the range of their munitions. The range for artillery projectiles can be extended by many methods [1]; increasing muzzle velocity of the projectile, boosted projectile by using rocket assisted or by improved ballistics which includes drag reduction or using sub-calibre projectile. The drag reduction can be obtained by two different ways. First, pressure drag reduction through improving projectile nose shape or by using projectile with long ogive part. Second, base drag reduction by enhanced boattail shape or increasing the base pressure to overcome the formed wake behind the projectile base. The most common method of increasing base pressure is using a base bleed (BB) unit conjugated to the projectile with boat tail as depicted in figure 1.

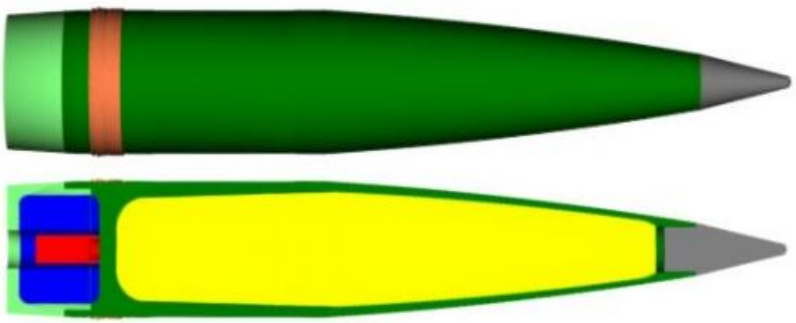

**Figure 1**. A boattail projectile with base bleed (BB).

The base bleed (BB) unit is formed from a propellant grain which is considered as gas generator. This grain may have many shapes such as slots, tubular, star and wagon wheel. The slotted split tubular grain shape is the most famous configuration it is used in 155 mm projectiles such as M864 K310 and K307 projectiles. The burning of base bleed works to increase the base pressure in the wake (under pressure zone) behind the projectile. This wake is generated when the separation of the turbulent boundary layer from the body at the projectile base occurs. The downstream flow passes by a strong expansion at the base corner forming a free shear which separates the outer in viscid flow forming large Primary Recirculation Region (PRR) downstream of the projectile base where mass is drawn from the recirculation region. Therefore, the pressure on the blunt base is reduced. When the base bleed is activated, the position of primary recirculation region shifts downstream due to the injected gases from the orifice of base bleed while a part of the gases escapes from bleeding section creating the so called Second Recirculation Region (SRR). The base pressure behind the projectile increases due to the mass added from the gases injected from the base bleed. Figure 2 shows a schematic drawing of a flow past a projectile with/out base bleed.

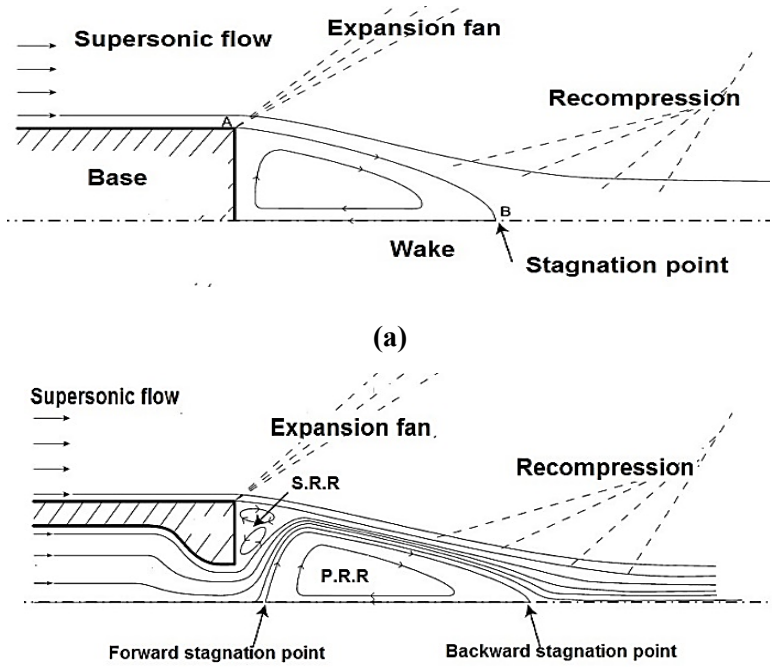


**Figure 2.** Scheme of a supersonic flow behind a blunt base (a) without BB (b) with BB [2].

Researches continue to this day on base drag reduction. Which can be obtained by two different ways. One of them is to increase the base pressure using active devices [3, 4] and /or passive devices [5-7] whereas, the other one is concerned with base drag reduction via boattailing [8]. There have been many trials to improve the ballistic performance of base bleed projectiles. The effect of the post-combustion of the base bleed grain on the base drag reduction was studied [9]. Also, it is confirmed that controlling the burning rate of the base bleed grain is an important factor to increase projectile range in the addition to the grain aging [10, 11]. Some studies examined different turbulent models to estimate drag coefficients of slender body with spin and base bleed [12]. Other studies proved that the nozzle pressure ratio of the base bleed unit has an influence on the drag reduction [13].

During developing projectiles with base bleed, it's to accurately estimate magnitude of drag reduction upon using base bleed. Drag on conventional projectiles can be estimated using engineering empirical methods computational techniques, wind tunnel tests, or live firings. However, for

projectiles with base bleed, no engineering empirical methods are available while wind tunnel test setup can be extremely complicated. Live firing is a reliable high-fidelity approach to estimate drag, however, it is expensive, time consuming, inflexible, and subject to design, production, and environmental uncertainties. Computational techniques based on CFD approach can be implemented to yield accurate prediction of drag on projectiles with base bleed. Being of a lower fidelity, computations need to be validated by comparing them with live firing counterparts.

A current research conducted by the authors is intended to examine novel designs of base bleed units based on computational simulations; validating the computational approach a necessary pre requisite.

The present study is carried out to a base bleed projectile model K307 to compare the calculations obtained from computational simulations with live firing measurements of drag coefficients at zero incidence. In addition, the computational approach is validated against available published firing results on the same projectile with and without base bleed unit. Based on results of this study, reliability of computational approach is assessed for further activities within the running research.

The remainder of the present paper is organized as follows. Details of the case study are explained next followed by study approach. Results are then presented and discussed and the paper finalized with the main conclusions.

## 2. Case Study

In this work, K307 projectile of 155 mm calibre with base bleed is studied and is manufactured especially for this purpose. Figure 3 shows the relative dimensions of the used projectile in terms of the calibre. A part from the 0.28D base bleed orifice, projectile dimensions are identical to original one. The mass of the projectile is about 46.5kg while the mass of the base bleed unit is 1.3kg.

This unit is consumed in 30seconds which implies that the flow rate of gases out of the base bleed unit is 0.045 kg/sec.

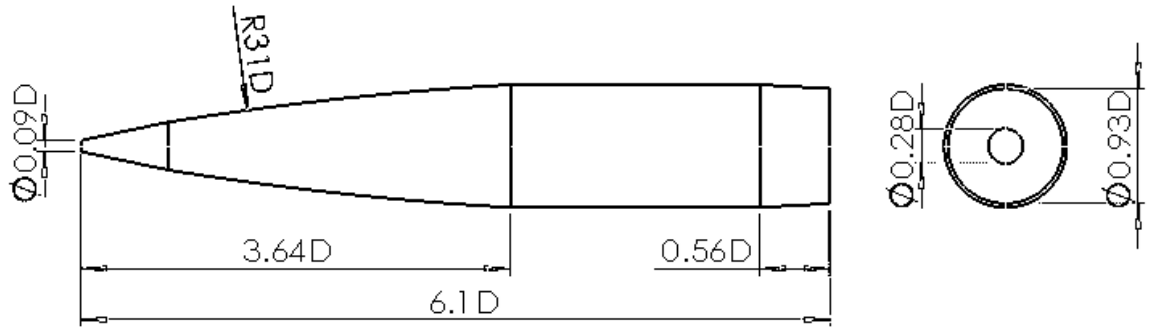


**Figure 3**. Relative dimensions of the projectile model in concern.

## 3. Methodology

### *3.1. Live firing experiments*

FiveroundsK307 projectiles with live BB are prepared to check their performance along trajectory in a certified Shooting Range facility. A 155mm caliber gun is used in the firing tests while a system of tracking consisting of a Mono-Pulse Doppler Antenna is used to capture the projectile position during flight on its trajectory, relative to the gun.

The trajectory parameters are calculated using a software installed to a computer interfaced with the tracking radar system. Inputs to the software include projectile mass, initial temperature, meteorological data, and firing angles. For the five rounds of the present study, firing angle is fixed at

45 degrees. The outputs of this system calculated by data acquisition and processing units are trajectory parameters including the variation of range, altitude, velocity with time till impact. Therefore, the drag coefficient $C_D$ can be estimated from the radar tracking data using many schemes as reported in Ref. [14].

*3.2. Computational Fluid Dynamics CFD approach*

Numerical simulations are conducted to estimate the drag coefficient on the projectile at zero incidence and different free stream Mach number values. Due to symmetry of both projectile and zero-incidence free stream, a one-eighth of the full 3D domain is constructed as shown in figure4. Boundary definitions are also shown.

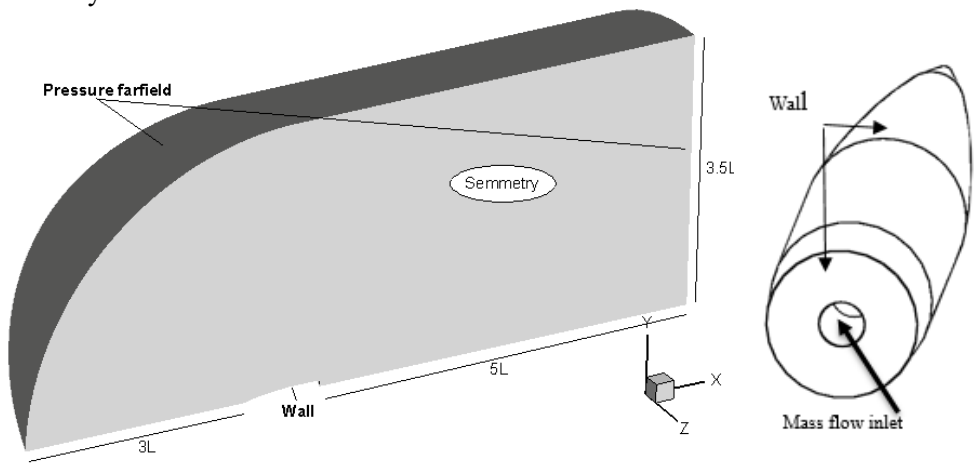


**Figure 4.** Computational domain and boundary condition.

The pressure far field boundary is set to the uniform upstream flow. The BB exit is defined as mass flow inlet with velocity satisfying the gases flow rate. The inlet flow conditions depend on the time and the position of the projectile along its trajectory [15]. The symmetric boundary is applied to the two side planes of the domain. The adiabatic no slip conditions are set to the solid projectile surfaces. Mass flow inlet boundary is defined at the base bleed orifice exit. The domain is extended in upstream up to 3L, 3.5L and 5L, respectively; L is the projectile length, lateral and downstream direction.

The domain is discretized into a structured grid with enhanced resolutions at the areas of interest, figure5.

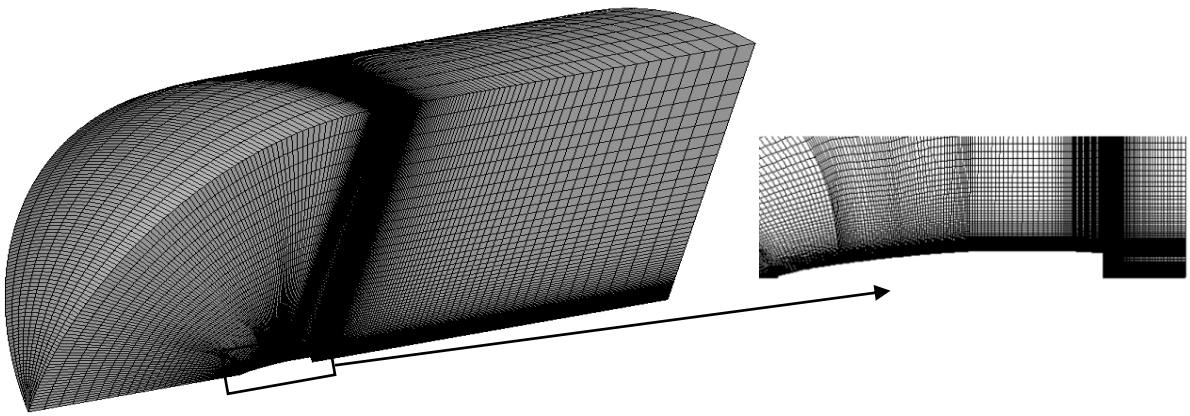

**Figure 5.** Structured 3-D grid (one-eighth domain).

Grid sensitivity study is done using 2-D version of the structured grids with different resolutions varying from 54300 cells to 85000 cells. Figure 6 shows the evolution of drag coefficient on the projectile unit grid size normalized by the size of the course one. The free stream for grid sensitivity check corresponds to Mach 1.5. A grid with 72300 cells is adopted since no significant improvement is attained with further increase in cell counts. This grid has 280 cells was distributed around the body (115 on ogive, 30 on cylindrical body, 50 on boattail and 85 on base), with about 140 cells upstream and above the model length and 200 cells downstream. Finally, the corresponding 3-D grid includes (714500 cells).

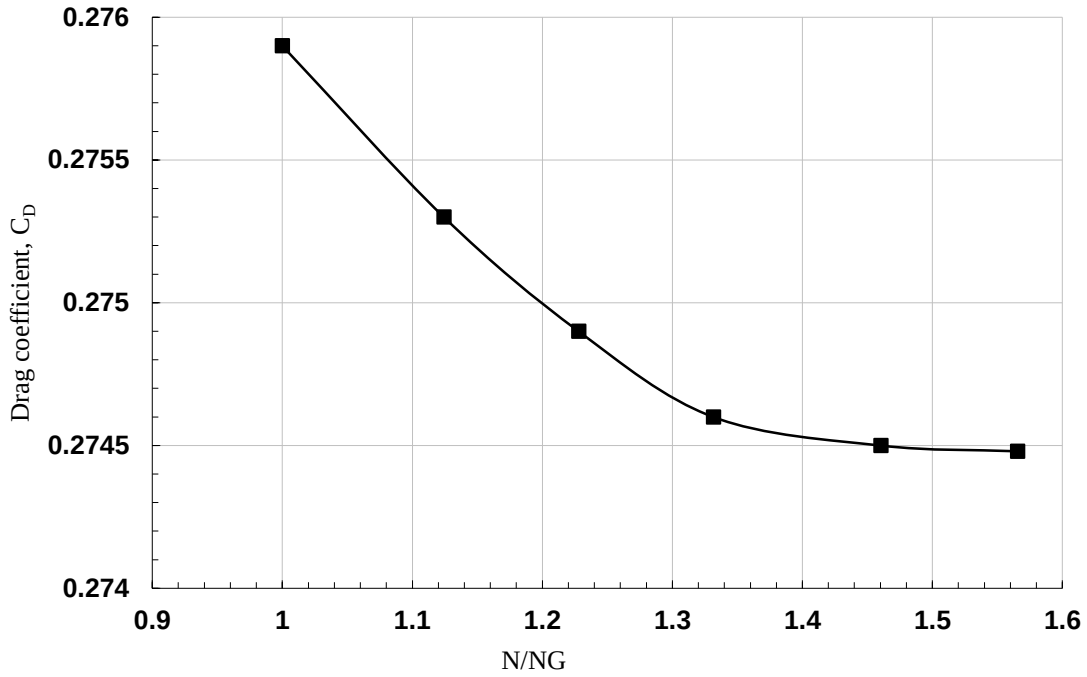


**Figure 6.** Drag coefficient versus normalized number of cells at M=1.5.

The implicit pressure base scheme is used to solve the system of differential equations. The second order upwind Green-Gauss node based scheme is also used in discretizing the spatial dependent variables in RANS equations. Coupled scheme is applied for pressure-velocity coupling. The turbulent model used in this work is K-epsilon Realizable Enhanced Wall Treatment. Air as an ideal gas is used as the working fluid for free stream flow. For base bleed gas flow, combustion products of base bleed change are defined with chemical reaction enabled [16].

## 4. Results and Discussion

### *4.1. Results of the live firing experiments*

Figure7 aggregates all drag coefficients for all rounds over the range of flight Mach number. The mean variation is also plotted. All values are listed in table 1.

*4.1.1. Comparison of the Computational simulations with published firing results.* The live firing measurements of total drag coefficient against Mach number carried out by Hwang and Kim [17] is chosen to validate the corresponding results of computational simulations in case of projectile with a dummy and active BB unit.

Figure 8 compares the published experimental measurements, computational results of the total drag coefficient at different Mach numbers for projectile K307 with dummy and live base bleed. Good

agreement is noticed between the CFD results of the drag coefficients with the published experimental measurements of the drag coefficient with difference less than 5.2% and 6.8% for dummy and live BB respectively. This is better shown in table 2.

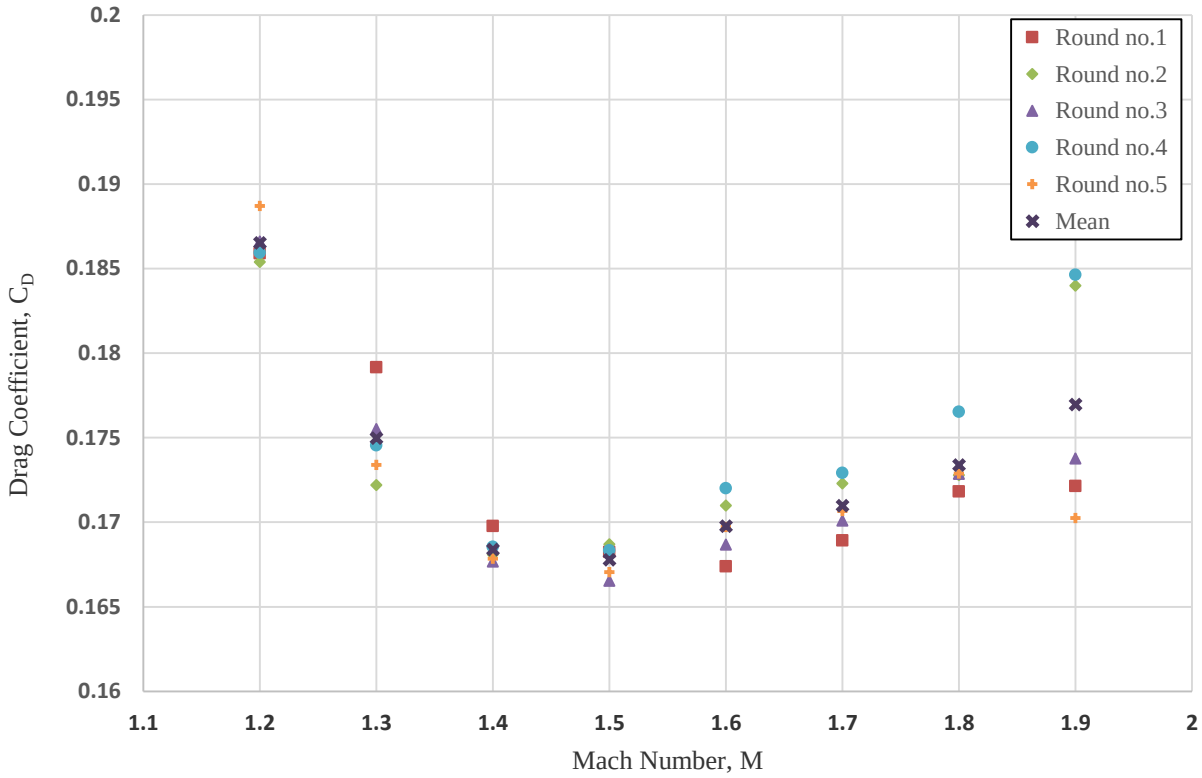


**Figure 7.** Drag coefficients versus Mach number for the live fired rounds.

**Table 1.** The measured drag coefficient for all rounds at all Mach number values.

| | 1.2 | 1.3 | 1.4 | 1.5 | 1.6 | 1.7 | 1.8 | 1.9 |
|---|---|---|---|---|---|---|---|---|
| 1 | 0.1859 | 0.1792 | 0.1698 | 0.1682 | 0.1674 | 0.1689 | 0.1718 | 0.1722 |
| 2 | 0.1854 | 0.1722 | 0.1681 | 0.1687 | 0.171 | 0.1723 | 0.1728 | 0.1839 |
| 3 | 0.1866 | 0.1755 | 0.1677 | 0.1665 | 0.1687 | 0.1701 | 0.1728 | 0.1737 |
| 4 | 0.1859 | 0.1745 | 0.1685 | 0.1683 | 0.1720 | 0.1729 | 0.1765 | 0.1846 |
| 5 | 0.1887 | 0.1734 | 0.1678 | 0.1670 | 0.1697 | 0.1706 | 0.1729 | 0.1702 |
| Mean | 0.1865 | 0.1750 | 0.1684 | 0.1678 | 0.1698 | 0.1710 | 0.1734 | 0.1770 |

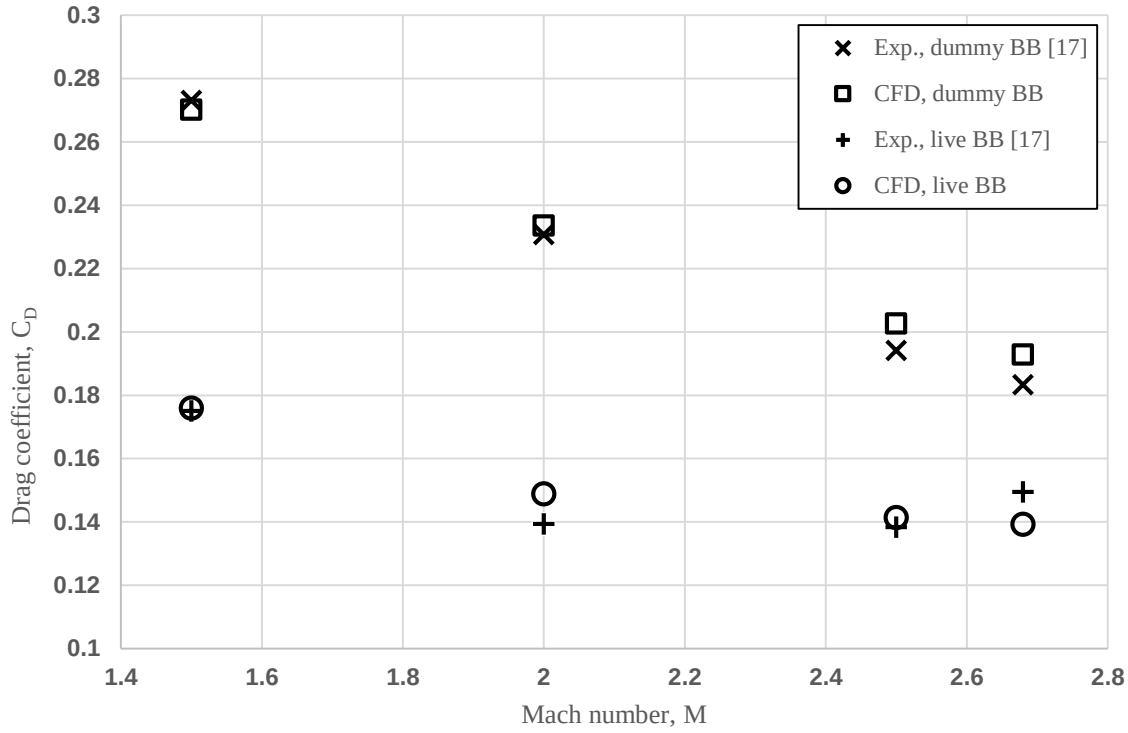


**Figure 8.** Experimental and computational drag coefficients versus Mach number for K307 with dummy and live BB.

**Table 2.** Experimental and computational drag coefficients result for K307 with dummy and live BB.

| M | With dummy BB | | | With live BB | | |
|---|---|---|---|---|---|---|
| | Exp. [17] | CFD | Difference (%) | Exp. [17] | CFD | Difference (%) |
| 1.5 | 0.2731 | 0.2701 | -1.1 | 0.175 | 0.1760 | 0.6 |
| 2 | 0.2307 | 0.2336 | 1.2 | 0.1394 | 0.1489 | 6.8 |
| 2.5 | 0.1941 | 0.2027 | 4.4 | 0.1384 | 0.1414 | 2.1 |
| 2.68 | 0.1833 | 0.1928 | 5.2 | 0.1495 | 0.1396 | -6.8 |

The impact of live BB is cleared from the previous table; we can notice that the drag reduction is about 18% to 40% when live BB used. The role of base bleed can be better understood by exploring the flow field features of the base of the projectile. Based on computational reproduction of the work of Hwang and Kim [17].

*4.1.2. Comparison of the Computational simulation with the live firing experiments.* Finally, the total drag coefficient measurements obtained from live firing test for five projectiles K307 with live base bleed grain are used to the computational results. Figure 9shows the computational results and the mean values of the experimental measurements of the total drag coefficient versus Mach number. The deviation between the computational results and the experimental measurements does not exceed

2.75%. Table 3 lists drag coefficient of the computational and the mean drag coefficients for the experimental work.

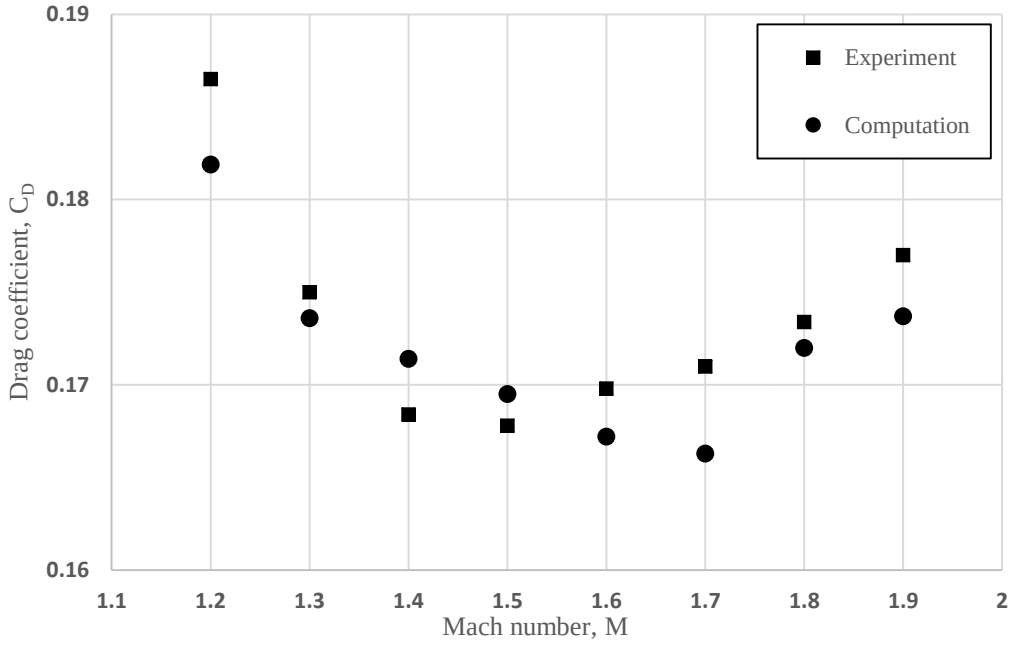


**Figure 9.** Experimental and computational drag coefficients versus Mach number (for projectile with live BB)**.**

**Table 3.** Experimental and computational drag coefficients for a K307 with live BB.

| M | Experimental (Mean value) | CFD | Difference (%) |
|---|---|---|---|
| 1.2 | 0.1865 | 0.1819 | -2.46 |
| 1.3 | 0.1750 | 0.1736 | -0.8 |
| 1.4 | 0.1684 | 0.1714 | 1.78 |
| 1.5 | 0.1678 | 0.1695 | 1.01 |
| 1.6 | 0.1698 | 0.1672 | -1.53 |
| 1.7 | 0.1710 | 0.1663 | -2.75 |
| 1.8 | 0.1734 | 0.172 | -0.81 |
| 1.9 | 0.1770 | 0.1737 | -1.86 |

## 5. Conclusions

- The objective of the present paper was to check the validity of computational simulation in predicting the drag on projectiles with base bleed. Simulations on K307 projectile were compared with published and the live firing results.
- The main conclusion of this paper is the acceptable drag coefficient values calculated by CFD compared with real firing test measurements. The used computational method could be applied for predicting the drag coefficients of developed projectiles with and without base bleed.

**References**

[1] Gurnners N E, Andersson K andHellgren R 1987 *Aeronautics and Astronautics Progress***16**(1) no 1 pp 537-61
[2] Kadic S S, Zecevic B, Terzic J and Catovic A 2012 *New Trends in Research of Energetic Materials* (Czech Republic: University of pardubice) part II pp 790-99
[3] Yu Wj, Yu Yg and Ni B 2014 *Defence Technology* **10**(3) pp 279-84
[4] Kubberud N and Ye I J 2011 *26th Int. Sympo. on Ballistics* (Miami: Florida)
[5] Ibrahim A Z and Filippone A2007 *Aircraft* **44**(6) pp 1865-76
[6] El-Awwad E, Ibrahim A Z,El-Sebaee A and Riad A2012 *15th Int. Conf. on Applied Mechanics and Mechanical Engineering*
[7] Suliman M A, Mahmoud O K, Al-Sanabawy M A and Abdel-Hamid O E 2009 *13th Int. Conf. on Aerospace Sciences & Aviation Technology* (Cairo Egypt: ASAT-13-FM-05)
[8] Cummings R M, Yang H T and Oh Y H 1995 *Computers & Fluids* **24**(4) pp 487-507
[9] Xiaochun X and Yonggang Y J 2016 *Applied Thermal Engineering* **109** pp 238-50
[10] Lingke Z Ruyuan Tand Zhuwei Z 2017 *Aerospace Science and Technology* **62** pp 31-35
[11] Zhang L K and Zheng X Y2018*Defence Technology* **14**(5) pp 422-25
[12] Péreza N, Velascob FJS, García JR, Otón RA, López A, Moratilla D, Rey F and Laso A2017 *Aerospace Science and Technology* **67** pp 126-40
[13] Longze M and Yonggang Y 2019 *Applied Thermal Engineering* **148** pp 502-15
[14] Dutta G, Singhal A, Kushari A and Ghosh A 2008 *Defence Science* **58**(3) pp 377-89
[15] Abou-Elela HA, Ibrahim AZ, Mahmoud OK and Abdel-Hamid OE 2013 *15th Int. Conf.on Aerospace Sciences & Aviation Technology* (Cairo Egypt: ASAT-15-207-AE)
[16] Marzouk O A and Huckaby E D 2010*Engineering applications of computational fluid mechanics* **4**(3) pp 331-56
[17] Hwang JS and Kim CK 1996*16th Int. Sympo. on Ballistics* (California; San Francisco) **2** pp 235-44